Atmos. Chem. Phys. Discuss., 10, 27135–27184, 2010
www.atmos-chem-phys-discuss.net/10/27135/2010/
doi:10.5194/acpd-10-27135-2010

Atmospheric Chemistry and Physics Discussions

Tropospheric ozone production related to West African city emissions during the 2006 wet season AMMA campaign

G. Ancellet[1], E. Orlandi[2], E. Real[1], K. S. Law[1], H. Schlager[3], F. Fierli[2], V. Thouret[4], C. Mari[4], and J. Leclair de Bellevue[1]

[1]UPMC Univ. Paris 06; Université Versailles St-Quentin; CNRS/INSU, UMR 8190, LATMOS-IPSL, France
[2]ISAC-Institute for Atmospheric Sciences and Climate, National Research Council, Italy
[3]DLR Institut für Physik der Atmosphäre, Oberpfaffenhofen, Germany
[4]Université de Toulouse, CNRS/INSU, LA (Laboratoire d'Aérologie, UMR 5560), France

Received: 1 September 2010 – Accepted: 2 November 2010 – Published: 10 November 2010

Correspondence to: G. Ancellet (gerard.ancellet@upmc.fr)

Published by Copernicus Publications on behalf of the European Geosciences Union.

Abstract

During the African Monsoon Multidisciplinary Analyses (AMMA) airborne measurements of ozone, CO and nitrogen oxides by the French and German falcon aircraft took place near three cities in West Africa (Cotonou, Niamey and Ouagadougou). Significant ozone production (O_3 increase of 40–50 ppbv) took place during two specific events: one near Cotonou on the coast of the Guinea Gulf, and the other near Niamey in the Sahel region. In both cases a high level of NO_x (>3 ppbv) is related to the ozone production. The ozone production is mainly driven by the Lagos-Cotonou anthropogenic emissions in Cotonou. In Niamey the combined effect of advection of VOC emissions from the forest and stagnation over the city area and the poorly vegetated soils recently wetted by convected systems is needed to achieve a similar level of ozone precursors. In Ouagadougou no ozone plume is found because of the absence of a pause in the convective activity and of the larger vegetated area around the city which prevented ozone plume formation during the wet season.

To discuss the ozone increase near Cotonou two different approaches have been implemented: a FLEXPART simulation to quantify the probability of transport from the SH compared to air mass stagnation over the emission area and a simulation of the BOLAM mesoscale model with two different tracers for the anthropogenic emission (RETRO inventory for 2000) and the biomass burning. The BOLAM model shows a good agreement with the meteorological observations of the aircraft and allows to identify the key influence of the anthropogenic emissions in the first 3 km while the biomass burning plume remains above this altitude.

The day to day variability of the ozone and CO in Niamey and Ouagadougou is discussed using FLEXPART simulations of the air mass stagnation in the 12° N–14° N latitude band and northward advection of air masses from the vegetated areas influenced by the biogenic volatile organic compound (VOC) emissions. Both conditions need to be fulfilled to be able to detect ozone increase within the city plume. The first condition is necessary to obtain a significant increase of the NO_x concentrations

ACPD
10, 27135–27184, 2010

by combining the city emission and the soil emission. It also shows that, contrary to the Niamey conditions, the Ouagadougou air mass transport and its timing respective to the convective activity did not correspond to favourable conditions for O_3 formation during the time period of the aircraft data.

Finally to check the magnitude of the ozone production related to the observed CO and NO_x observations, a 2-days stationary run of the CittyCAT Lagrangian model was conducted at Cotonou location. The initialisation of the chemical concentrations not measured is done by scaling to the NO_x and CO concentrations observed in the polluted plume. The scaling factor is derived from the low altitude observations provided by the DF20 and the BAe-146 aircraft during the AMMA campaign. Under such conditions, the simulation show that 50 ppbv of ozone can be produced in a 2-days period.

1 Introduction

According to UNEP, Africa will have the fastest growth rate in the world between 2000 and 2050, twice the rate of any other region during that time. Given their relatively low industrial development, air pollution in west African countries is not as widespread as in other regions of the world. However, in most populous cities, long-term exposure to poor-air quality has been found to become a severe health issue for the population. Africa is also known to contribute to ozone formation at the global scale mainly because of large amounts of biomass burning (Andreae and Merlet, 2001; Thouret et al., 2009), biogenic emissions (soil and vegetation) (Guenther et al., 2006; Huntrieser et al., 2008) and lightning NO_x (Schumann and Huntrieser, 2007). The anthropogenic emissions related to fossil fuel combustion are generally considered as a regional problem (Aghedo et al., 2007). For example large cities like Lagos (6°35′ N, 3°2′ E) along the coast of the Guinea Gulf are known to influence air quality and ozone production at local scale (Baumbach et al., 1995; Minga et al., 2010). Most recent emission data bases still underestimate this contribution for an accurate modelling of the aerosol and trace gas distributions (Liousse et al., 2010).

ACPD
10, 27135–27184, 2010

Although many papers discuss the link of tropospheric ozone total column variability over West Africa and tropical Atlantic with biomass burning emissions (Thouret et al., 2009; Sauvage et al., 2007b; Thompson et al., 2000), there are few papers about city plume studies in this region. Minga et al. (2010) showed that during the dry season very large ozone amount can be found near Cotonou (2°26′ E, 6°60′ N) due to the Lagos industrial area. Hopkins et al. (2009) also discussed the impact of the city of Lagos on ozone precursor emission using the data of a BAe-146 UK aircraft recorded during a circular flight around the city in July 2006. The emission levels for NO_x and CO are found to be high enough to characterise the Lagos area as a polluted megacity, but the fate of these emissions for photochemical ozone production is not discussed in this study. Ozone production due to African megacities then remains poorly documented especially during the wet season.

In this paper, our objective is to analyse aircraft data collected near three major cities: Cotonou, 2°26′ E, 6°60′ N, Niamey, 2°05′ E, 13°32′ N and Ouagadougou, 1°32′ W, 12°22′ N, focusing on ozone production and the respective impact of anthropogenic emission and SH biomass burning. Aircraft data has the great advantage of providing vertical profiles of O_3 and its precursor gases, namely NO_x and CO. The aircraft have been deployed during the African Monsoon Multidisciplinary Analyses (AMMA) campaign held in July-August 2006 for studying the role of convection on the atmospheric composition (Reeves et al., 2010). During the wet season, O_3 photochemical production in the lower troposphere is known to be limited by frequent fast vertical mixing (Chatfield and Delany, 1990), but it provides a better altitude decoupling of the respective influence of biomass burning and African cities emissions on the regional ozone production. Thouret et al. (2009) indeed show that the advection of biomass burning from the Southern Hemisphere (SH) during the wet season is seen at higher altitudes (3–5 km) than during the dry season (1–3 km).

The paper is structured as follows: In Sect. 2, we recall the meteorological context and differences between Cotonou on one hand and Niamey/Ouagadougou on the other hand. In Sect. 3, the aircraft observations are presented and discussed. In Sect. 4,

ACPD
10, 27135–27184, 2010

the air mass transport is studied using Lagrangian model simulations (FLEXPART), namely to identify whether air masses stay long enough under the influence of the city emissions or are influenced by other emissions (Southern Hemisphere, tropical forest). In Sect. 5, the vertical structure of the ozone observations in Cotonou is compared to modelling work: a tracer simulation with the mesoscale model (BOLAM) to separate anthropogenic and biomass burning emissions and an ozone simulation with a chemical box model (CittyCAT) using the aircraft observations. which can be produced in a typical polluted city plume.

2 Meteorological context and characteristics of the selected cities

The synoptic situation over West Africa is characterised by the convergence of the Harmattan and the monsoon fluxes. Figure 1 illustrates the main averaged characteristics of these flows in the 0–1 km, 1–3 km and 3–4 km layers during August 2006 based on the ECMWF reanalysis with assimilated AMMA soundings (Agusti-Panareda et al., 2009). Below 3 km, the Guinea coast and Cotonou are under the influence of the humid and relatively cold monsoon flux from the south-west. Below 1 km the monsoon flow penetrates inland reaching Ouagadougou (Burkina Faso) and Niamey (Niger). Above 3 km, the most streaking feature is the northern African Easterly Jet (AEJ-N), located north of 10° N, with wind speed over 15 m/s (Parker et al., 2005; Tompkins et al., 2005). The southern African Easterly Jet (AEJ-S), with wind speed up to 9 m/s, advects emissions from the Southern Hemisphere (SH) to the equatorial Atlantic. The AEJ-S also shifts northward as it crosses the Equator above the Atlantic ocean. Although much weaker than the AEJ-N, the AEJ-S then plays an important role in the inter-hemispheric transport of biomass burning pollution (Mari et al., 2008). The role of the monsoon circulation on the regional ozone and CO distribution is discussed in Reeves et al. (2010), and in this paper we only consider the meteorological factors important for O_3 production resulting from anthropogenic emissions.

ACPD
10, 27135–27184, 2010

According to the weather patterns in the lower troposphere, we must distinguish two groups of cities: (i) Lagos or Cotonou mainly influenced by SH emissions and the Atlantic boundary layer chemical composition, (ii) Niamey and Ouagadougou, named hereafter the Sahelian cities which are mainly influenced by the northernmost part of the monsoon flow advecting biogenic emissions from the forest. This is why we will analyse separately the Cotonou observations and the Niamey/Ouagadougou data set. Even though Niamey and Ouagadougou are similar with respect to the weather patterns, we expect different emission factors for these two cities considering their different population sizes (1.2 million for Ouagadougou and 700 000 for Niamey). During the wet season, numerous mesoscale convective systems (MCSs) can developed over West Africa with a strong impact on vertical mixing of O_3 and O_3 precursors. This is known to impact the ozone distribution over the whole troposphere, but also to control the timing of the low level ozone production. This parameter must be analysed when discussing the data set.

3 Aircraft data analysis

3.1 The data set

The measurements used in this paper were recorded by the French and German Falcon aircraft (named FF20 and DF20 hereafter) when they flew at altitudes less than 3 km just after takeoff or before landing in one of the West African cities. The FF20 data were obtained near Cotonou (2 profiles) and near Niamey (11 profiles), while the DF20 data were collected near Ouagadougou (16 profiles). The chemical species discussed in this paper are mainly O_3, CO and NO_x measurements. The specific humidity is also used to described the PBL structure, especially its diurnal evolution between takeoff and landing profiles. The FF20 and DF20 instruments are respectively described in (Ancellet et al., 2009) and in (Baehr et al., 2003). The NO_xinstrument on the FF20 experienced problems with an ozone leak during the AMMA campaign and NO_x was only

ACPD
10, 27135–27184, 2010

measured in Cotonou (2 profiles) and near Niamey on 19 and 20 August (4 profiles). The FF20 CO measurements require frequent zero monitoring and only 8 out of the 11 profiles are available near Niamey because the zero monitoring occurred during the aircraft landing. The DLR falcon did not measure NO_x concentration, but NO. Since it is important to make the Ouagadougou data set comparable to the Niamey data, we have estimated the NO_x from the measured NO and O_3 concentrations assuming that (i) the NO_x partitioning is only determined by the NO_2 photolysis and NO + O_3 reaction (ii) the NO_2 photolysis coefficient is of the order of 0.015 s^{-1}. There is a 20–30% uncertainty in the NO_x values but good enough to discuss the occurrence of polluted layers with high NO_x values.

The dates and times of the available profiles near Niamey and Ouagadougou are summarised in Tables 1 and 2. In both cities, 6 O_3 profiles are obtained after 14:00 UT, i.e. when an O_3 plume is more likely to be detected considering the strong diurnal cycle controlling the ozone concentration in the PBL. This corresponds in both cases to 4 different days. So the two data set are quite comparable as far as O_3 sampling is concerned.

3.2 Analysis of the Cotonou observations: a city on the southern coast

Before discussing our aircraft observations, let us analyse the lowest altitude range (0–2.5 km) in the 24 ozone sondes record presented in Thouret et al. (2009), which corresponds to the overall 2006 wet season. Ozone concentrations larger than 50 ppbv at altitudes below 2.5 km are not very common in this data set. The 2006 summer mean ozone profile and the data for the sonde launched on 17 August 2006, (i.e. two days before the aircraft measurement) have a similar structure showing a positive ozone vertical gradient, but with ozone concentrations exceeding 50 ppbv only at altitude above 3 km (Fig. 2). It is related to the biomass burning plume advected from the SH (Mari et al., 2008), as illustrated by the ozone peak observed at 3.5 km on 17 August. Low ozone values (75 percentile at 30 ppbv) near Cotonou 6° N below 750 hPa are also discussed in Reeves et al. (2010) showing the role of the weak ozone production over the

ACPD
10, 27135–27184, 2010

ocean and the strong ozone sink over the vegetation area inland. Since the Cotonou ozone sonde launch site is located west of the city centre, it is more influenced, at low altitudes, by the southerly flow advecting air poor in ozone from the ocean. This is shown by the 30 June sounding, which is the only one in this record with a significant O_3 increase in the monsoon layer below 3 km (Fig. 2). Low level wind data indeed indicates an easterly flow for this day suggesting advection of the Cotonou city plume or even more eastward emissions from Lagos which are responsible for higher the O_3 concentrations with respect to the seasonal mean.

Aircraft observations of CO and O_3 offer another way to analyse the potential impact of anthropogenic pollutants when using vertical profiles east and west of the city of Cotonou. The aircraft data also offers the possibility to address the question of ozone production more precisely by using the vertical profiles of CO and NO_x. On 19 August 2006, the FF20 aircraft made a landing at 12:00 UT and a takeoff at 13:45 UT in Cotonou. The aircraft position around the city of Cotonou is shown on Fig. 2 when exploring the 0–3 km altitude range. Considering the small time difference between the two corresponding vertical profiles, the comparison provides a good estimate of the local scale gradients across the coast: southwest-northeast gradient below 3 km and northwest-southeast gradient above 3 km. A dropsonde launched when flying over Cotonou at 10:41 UT (Fig. 2) provides the observed wind vertical profile and the boundary layer structure using the water mixing ratio. The most remarkable feature looking at the difference between the east and west ozone profiles is the significant O_3 increase (+50 ppbv) in the 1–3 km altitude range with concentrations reaching 80 ppbv East of Cotonou (Fig. 3). The water vapour mixing ratio profiles from the aircraft and the dropsonde show that the monsoon layer height extends up to 2.5 km and that it does not change very much during the time period 11:00 UT to 14:00 UT and over the spatial domain corresponding to the aircraft measurements. So such a difference in the ozone is not related to a sharp discontinuity of the boundary layer height as observed sometimes near a coast line. Notice also that below 1 km and above 3 km, the change in the ozone vertical distribution is completely different. The large ozone values above 3 km

ACPD
10, 27135–27184, 2010

are now observed in the whole area above the coastline and are known to be related to advection of biomass burning from the SH (Mari et al., 2008). The effect of these emissions on O_3 are already seen above 2.5 km in the ozone sonde profile taken on 17 August (Fig. 2). When the aircraft approaches the city by the North, O_3 concentrations at altitudes below 1 km for the east profile are as low as the 1- to 3-km O_3 values in the west profile (20 ppbv). On the contrary O_3 at altitudes below 1 km in the west profile increases to values near 50 ppbv when the aircraft becomes closer to Cotonou. The black line of Fig. 2 then represents the limit between the areas with high (East of the line) and low (West of the line) O_3 concentrations.

Looking now at the corresponding CO and NO_x vertical profiles (Fig. 3), they also indicate larger CO (up to 250 ppbv with a 100-ppbv increase) and NO_x (up to 5 ppbv with a 3-ppbv increase) concentrations for the east sector. Notice that the shorter lived compound, NO_x, followed more closely the structure of the boundary layer with a sharp gradient at 2.5 km. The CO vertical profile is more comparable to the ozone profile. The ozone increase across the line of Fig. 2 then corresponds to a concentration build-up longer than the daily timescale of the boundary layer height evolution. Above 3 km, the weak northwest-southeast CO gradient is consistent with the role of the biomass burning emissions on O_3 concentrations. Below 1 km, the NO_x relative increase up to 2.5 ppbv as the aircraft approaches again Cotonou (see Fig. 2) suggests that the 50-ppbv ozone concentrations in the lowest altitude range of the west profile are indeed related to the increase of the coast line emissions. Notice also that the wind profile measured by the dropsonde shows a southwesterly direction of the monsoon flow explaining the Southwest/Northeast direction of the limit between the polluted and unpolluted air in Fig. 2. There is also a layer of weak wind between 1 and 2.5 km which probably maintains the coast line emissions near Cotonou in this altitude range.

To address more explicitly the question of the respective influence of the emissions from the cities along the Coast, namely Cotonou and Lagos and of the biomass burning products advected aloft at altitudes higher than 3 km, we need a more detailed analysis of the transport mechanisms. Before discussing this part of our work, it is important

ACPD
10, 27135–27184, 2010

to study similar measurements near the two other cities less influenced by the SH emissions.

3.3 Analysis of the Niamey and Ouagadougou observations: Sahelian cities

The median, 25th and 75th percentile of the CO and water vapour vertical profiles recorded in Niamey shows a daytime PBL extending generally up to 1.2 km (Fig 4). Although the PBL structure does not change very much from one day to the next, there is a significant variability in the CO concentration with 25% of the distribution above 200 ppbv and below 120 ppbv within the PBL. This indicates that the city emission is not large enough to maintain a constant high CO level as observed near the coast. Nevertheless flights within polluted plumes occurred as shown by the occurrence of high CO values. The ozone values are generally lower than 35 ppbv just above the PBL as discussed in Reeves et al. (2010) for this altitude range, but are higher (median value at 45 ppbv) within the PBL (Fig. 5). This is very different from Cotonou where there is a positive ozone gradient. It suggests that photochemical production occurs within the PBL and that the ozone depleted air is only found above 1 km. The day to day variability of the O_3 and CO concentrations is also shown in Fig. 5. The days with the largest probability of sampling the Niamey plume, i.e. with the largest CO values, are encountered during the period 15 August to 17 August. One day (on 16 August) shows a clear ozone plume with concentrations up to 70 ppbv between 0.5 and 1 km during the descent. Therefore an ozone production, as large as for the case recorded in Cotonou, may also occur around Niamey. More high O_3 episodes were not observed probably because very specific conditions are required like an air mass stagnation around the city or a significant addition of NO_x by wetted bare soil emissions as discussed by Saunois et al. (2009) using a regional model and observations. The role of the transport in the observed day to day variability is discussed more precisely in Sect. 4.

To quantify the possible positive O_3 production on 16 August 2006, we unfortunately do not have NO_x concentrations measured by the FF20, but NO_x was measured by the aircraft on 19 and 20 August (Fig. 6) with values of the order of 3 ppbv in the afternoon

ACPD
10, 27135–27184, 2010

in the upper part of the PBL. We then can expect even higher NO_x values for the days corresponding to the polluted plume crossing (15 to 17 August). The morning NO_x profiles with concentrations in the 0.5–1.5 ppbv range, should be representative of the background NO_x concentrations and are in fact quite similar to the BAe-146 aircraft average NO_x vertical profile near Niamey (Saunois et al., 2009). Such NO_x concentrations are primarily due to NO emissions from recently wetted soil (Huntrieser et al., 2008). This will be dependent on the MCS development in the 12°–15° N latitude band which is reported in Table 3. The convective activity is maximum in the first half of August and slows down at least over Western Niger only after 14 August. So indeed soil NO_x emissions can be still significant during the period 15 August to 17 August and can be added to emissions from the city of Niamey to increase NO_x concentrations to values nearly as high as in Cotonou (i.e. of the order of 5 ppbv). In addition after 14 August, reduction of local cloudiness and precipitation will maintain high level of NO_y, HCHO, NO_2 photolysis and production of HO_x radicals. This would explain the observed ozone increase of 30 ppbv in a 2 day period in the polluted plume observed on 16 August. To explain the low ozone values observed again on 17 August, on can notice that the new convective activity on this day (Table 3) limits further O_3 plume formation even though the aircraft still measures high CO values.

A similar analysis is conducted for the Ouagadougou flights of the DF20. The CO and NO_x profiles show again a PBL reaching 1.2 km, but elevated CO (>200 ppbv) are only observed below 700 m near the ground (Fig. 7). The CO variability (i.e. the difference between the 25th and 75th percentile) is also less than in the Niamey data set. This is a good indication that CO is quickly mixed and that no well defined polluted plumes advected away from the city at altitudes above 700 m are encountered by the aircraft. The largest NO_x concentrations of the order of 1.5 ppbv above 700 m are also less than the Niamey values. This NO_x concentration can be explained by the 12°–16° N biogenic sources discussed in Huntrieser et al. (2008) without necessarily a significant addition of NO_x by the city emissions. Looking at the 25th, 50th and 75th vertical ozone profiles (Fig. 8) there is a small variability around 30 ppbv, which is consistent with less ozone

ACPD
10, 27135–27184, 2010

produced by polluted plumes. The positive O_3 vertical gradient is also quite different from the Niamey data set and corresponds to the ozone sink by a larger vegetated area around Ouagadougou. Notice also that according to Table 3, most of the DF20 flights took place during the very active convective period increasing mixing and preventing ozone production. The daily variability of the O_3 or CO concentrations (Fig. 8) confirms that no particular day with condition favourable to pollution plume formation and ozone production have been recorded.

To summarise, the Sahelian cities can exhibit also ozone production in the city plumes. Differences in the anthropogenic emissions between Ouagadougou and Niamey should lead to more polluted case studies for the former. This is not the case, so other factors must drive the differences in the variability of this kind of O_3 production:

1. the timing of the convective activity since the significant O_3 production in the city plume occurs during a non convective period to reduce mixing and wet removal processes, but following a very active one necessary to increase NO_x soil emissions.

2. the vegetation cover since the local ozone sink is more efficient to remove O_3 over the more vegetated city (Ouagadougou).

Different transport mechanisms may also be responsible for the daily variability observed in both places and for the difference of the ozone production efficiency in Niamey and Ouagadougou. In the following section we address these issues.

4 Transport of the air masses

4.1 Cotonou case study: 19 August

The FLEXPART model version 6 (Stohl et al., 1998, 2002) driven by 6-hourly ECMWF analyses (T213L91) interleaved with operational forecasts every 3 h, was run for 5 days in a backward mode by releasing 2000 particles in 2 boxes at 2250 m and 3750 m. The

ACPD
10, 27135–27184, 2010

box depths are 500 m and their horizontal extent are 1°×1°around the city of Cotonou. FLEXPART is used with ECMWF analysis with 91 model levels and a resolution of 0.5°. The initial version of the model includes the computation of potential vorticity (PV) for each air parcel. The fraction of particles with PV>2 PVU (1 PVu = 10^{-6}K kg^{-1} m^2) is calculated for each time step to estimate the probability of transport from or into the stratosphere. Previous studies have shown that a fraction larger than 20% encountered during a 5-days time period corresponds to a significant influence of the stratosphere-troposphere exchange (STE) for the air mass at the release time (Colette and Ancellet, 2006). We modified the FLEXPART model to introduce the calculation of the fraction of particles originating below an altitude of 3 km, for two areas corresponding to different emissions of ozone precursors and CO: the SH (latitude <0° N, longitude <40° E) for the biomass burning emission, a 1° latitude band along the coast line of the Gulf of Guinea (latitude ∈[6° N 7° N]) for the anthropogenic emissions. The upper troposphere-lower stratosphere (UTLS) fraction is defined as the particles coming from altitudes above 8 km and latitudes >8° N. These fractions are shown as a function of time in Fig. 9. For the layer with a release at 2250 m, i.e. corresponding to the layer with the ozone positive gradient from Southwest to Northeast, the fraction of particles remaining in the coastal region is high for at least 3 days, while the transport from the SH remains weak (fraction <10%) even after 5 days. For the layer above 3 km, local emissions near the coast have little influence compared to biomass burning emissions from the SH, even though the fraction from the SH remains of the order of 10%. Therefore the FLEXPART simulation shows that the low level southwest/northeast positive ozone gradient is largely related to local emissions near the coast.

4.2 Niamey and Ouagadougou observations

FLEXPART was also run in a backward mode for two boxes located above Niamey and Ouagadougou at an altitude of 1 km. We again release 2000 particles in 500 m×1°×1° boxes. The fraction being at a given time step in two specific regions are also calculated: a 1° latitude band around Niamey or Ouagadougou and the area with more

ACPD
10, 27135–27184, 2010

vegetation, i.e. with latitude <10°. A large fraction in the first region points to a possible combined influence of local anthropogenic emissions and soil NO_x emissions provided that the stagnation takes place after a convective period. A large fraction in the second region is useful to discuss how advection of biogenic emissions from the forest may change the ozone production (e.g. by increasing isoprene or terpene plant emissions and by changing the HO_x radical chemistry). The enhancement of ozone production in a city plume at mid-latitudes was indeed observed when the plume mixes with background air strongly influenced by biogenic species (Derognat et al., 2003). The daily variability of the FLEXPART fraction of particles staying in the 1° latitude band around the city and the fraction of particles influenced by the land emission south of 10° N are reported in Fig. 10. The city latitude band fraction is given 24 h before the release as it is the minimum time period to obtain a measurable ozone production when influenced by city emissions. The southern region fraction is given 48 h before the release as longer time period reduces the lifetime of the ozone precursors from biogenic emission.

For Niamey results show that there are 4 days with afternoon fractions >20% in the city latitude band (11, 15, 16, and 17 August). Afternoon observations are more likely to correspond to higher ozone values when photochemistry is more active within the PBL. Regarding advection of southern air masses, it is only significant for the time period after 14 August (>30%), except for 15 August. There are then 2 days with a stagnation of the air mass near Niamey following a northward advection: 16 and 17 August. The latter corresponds to very cloudy conditions in the afternoon due to convective activity (Table 3) reducing HO_x radicals and removing NO_y. Therefore the optimum air mass transport conditions for O_3 production are expected on 16 August which shows indeed the largest ozone plume.

For Ouagadougou, there are only 2 days with the afternoon fraction remaining >20% for 24 h in the city latitude band (1 and 11 August). But these days are also for time periods where there are the smallest northward transport and the passage of an MCS with frequent overcast and mixing during the day. The influence of advection from

ACPD
10, 27135–27184, 2010

latitudes <10° is often very high and even dominates the air mass composition on 4th and 6th August. This makes the Ouagadougou averaged vertical profiles more representative of photochemical conditions found above the forest and with less impact of the city emissions but also of the wetted bare soil NO_x emissions. It is consistent with the absence of strong ozone values and the moderate NO_x concentrations of the DF20 flights compared to the Niamey FF20 flights.

While local ozone deposition and convective influence play a role in the differences between Niamey and Ouagadougou observations as explained before, one see that the transport mechanisms is also more favourable for the occurrence of ozone rich plumes near Niamey. It means also that the observed differences are only valid for the conditions encountered during the campaign. Ouagadougou consequently could be also influenced by high ozone plume provided that the right transport pathways and convective conditions are fulfilled.

5 Modelling of the Cotonou case study

The objective of this section is to demonstrate on one hand that regional ozone production related to the SH biomass burning is indeed lower than the O_3 source from local city emissions, and on the other hand, that the chemical composition is consistent with an O_3 increase of the order of 50 ppbv in two days. The first objective needs to reproduce the detailed dynamical processes of the monsoon layer, i.e. a simulation by a mesoscale model. The advantage of the mesoscale model for addressing the complex interaction of emissions and dynamics in the monsoon layer has been demonstrated by several studies (Vizy and Cook, 2002; Sauvage et al., 2007a; Delon et al., 2008). The second objective can be estimated as a first guess by a chemical box model initialized by observations. A similar approach was used in the Minga et al. (2010) work with a 0D chemical model to study the ozone production downwind of Lagos.

ACPD
10, 27135–27184, 2010

5.1 Mesoscale modelling of the biomass burning and anthropogenic emission transport

5.1.1 Mesoscale model description and simulations setup

BOLAM (BOlogna Limited Area Model) is a limited-area meteorological model based on primitive equations in the hydrostatic approximation. Prognostic variables (horizontal wind components, potential temperature, specific humidity and surface pressure) are defined on hybrid coordinates and are distributed on a non-uniformly spaced Lorenz grid. It includes a microphysical scheme that has five prognostic variables (cloud water, cloud ice, rain, snow and graupel), as derived from the one proposed by Schultz (1995). Deep convection is parameterized with the scheme of Kain-Fritsch (Kain, 2004). Vertical diffusion is modelled using the mixing-length assumption and the explicit prediction of turbulent kinetic energy (Zampieri et al., 2005). Further details of the model are provided in Malguzzi et al. (2006).

Here the mesoscale model BOLAM is used to simulate the transport of southern hemispheric biomass burning and regional anthropogenic emissions in West Africa. To take into account the different spatial and temporal scales involved in the transport, two simulations have been performed: a three month one for biomass burning emissions and a shorter and higher resolution one for anthropogenic emissions. For both simulations ECMWF AMMA re-analyses (Agusti-Panareda et al., 2009) have been used as initial and boundary conditions.

1. The biomass burning emissions simulation (hereafter 24 km-bb) characteristics are the following:
   The simulation starts on 15 June and ends on 31 August 2006. Meteorological fields have been re-initialized on 1 July and 1 August. The horizontal grid resolution is $216^{\circ} \times 216^{\circ}$ (around 24×24 km) and 38 vertical levels are used. The domain includes both West Africa and the area of SH wild fires, domain's limits are longitude=[−22.40] and latitude=[−20.29]. The tracer has been injected up

ACPD
10, 27135–27184, 2010

to 1 km altitude and 5-days averaged CO emissions from the biomass burning emission inventory described in Liousse et al. (2010), have been used for the horizontal distribution of the tracer. An exponential decay has been imposed to the tracer with a lifetime of 20 days (reasonable for CO as discussed in Mauzerall et al. (1998)).

2. Local anthropogenic emissions simulation (hereafter 7 km-anthro) characteristics are the following:
The simulation covers a period of 5 days, starting on 00:00 UTC of 15 August, 2006. The horizontal grid resolution is 07°×07°(around 8×8 km) and 60 vertical levels are used with 21 levels below 3 km and the lowest level at 65 m. The domain's limits are longitude =[−2.8, 7.6] and latitude=[1.1, 11.5]. The tracer field has been initialized to zero and CO fluxes from the RETRO inventory at 5° resolution and a monthly time resolution for year 2000 (http://retro.enes.org/) are used to inject the anthropogenic emissions in the lowest model layer during the whole simulation. The horizontal distribution of the tracer is based on the map of the CO fluxes shown in Fig. 11. Black and red asterisks in Fig. 11 indicate the position of the cities of Lagos and Cotonou. Close to Lagos high value for emissions are reported, while the overall area encompassing Cotonou and Lagos exhibits weak emissions (below 1 µg/m^2/s). As for the case of biomass burning, an exponential decay with a lifetime of 20 days have been imposed on the anthropogenic tracer. Even if an exponential decay have been imposed and CO emissions have been used, biomass burning tracer is reported in arbitrary unit instead of ppbv of CO because the simulation is too long to neglect chemistry.

5.1.2 Tracer simulation results

Figure 12 shows the vertical profile of wind speed and wind direction measured by the dropsonde launched at 10:41 UTC by the FF20 and simulated in the 7 km-anthro simulation at 10, 12 and 14:00 UTC above Cotonou. Measurements show the monsoon

ACPD
10, 27135–27184, 2010

layer with a uniform southwesterly wind from ground up to 1.2 km and wind speed with a maximum of 10 m/s at 5 km and decreasing toward 0 m/s at 1.2 km. BOLAM (black line, 10:00 UTC) reproduces such a layer, underestimating the maximum wind speed. Above the monsoon layer, measurements report a counter-clockwise rotation of 360°of the wind between 1.2 and 2.5 km and then again a south-westerly wind from 2.5 km upward. BOLAM model is able to reproduce the vertical variation of the wind direction and the overall vertical structure of the wind, even if it underestimates wind speed above 2 km and, due to the finite vertical resolution, is not able to catch the sharp increase in wind speed at 2.1 km.

Figure 13 shows the relative humidity measured by the FF20 dropsonde and the time evolution of the vertical profiles of relative humidity and tracer concentration for the 7 km-anthro simulation above Cotonou. Both measured and modelled relative humidity shows a boundary layer extending up to 1.9 km with a nearly saturated atmosphere and a sharp decrease toward a value of 30% at 2.5 km. The time evolution of the anthropogenic tracer concentration profiles shows high values at the ground, were there are emissions of CO, and a minimum around 0.9 km due to the southwesterly advection of air with low tracer concentrations from the ocean. Above the minimum and up to 2.8 km, a tracer layer with maximum around 2.4 km is visible, in agreement with O_3 and CO profiles influenced by Cotonou city plume (west profiles in Fig. 3).

Figures 14 and 15 report the horizontal distribution and the vertical cross section of anthropogenic tracer concentration from 7 km-anthro simulation. The solid line in Fig. 14 shows the position of the vertical cross section in Fig. 15. Horizontal cross section shows that the anthropogenic tracer is transported from emission region along the coast (pink squares in Fig. 14) through North-East by the monsoon flow. Highest concentration are related to Lagos emissions. The vertical cross section of tracer concentration in Fig. 15 exhibit a strong South-West North-East gradient with Cotonou on the boundary of the area influenced by anthropogenic emissions, supporting the thesis that the FF20 made measurements into regions with different characteristics on takeoff and landing.

ACPD
10, 27135–27184, 2010

In Figure 16 the horizontal distribution of biomass burning tracer from 24 km-bb simulation at 900 hPa is presented. It can be seen that around Cotonou (red asterisk in Fig. 16) the tracer remains confined far from the coast. The vertical structure of the tracer over Cotonou (red asterisk) shows that a layer of high concentrations is present from 2.5 km upward. This structure agrees with our observations and also the work of Thouret et al. (2009) that reports frequent ozone enhancements above Cotonou between 3 and 5 km in August 2006. At lower altitude, the tracer remains confined far from the coast in the simulation in agreement with the observations above the ocean, but we must take into account the known difficulties of models transporting SH fire tracers at low altitude levels near the West African coast (Williams et al., 2010).

5.2 Modelling of the ozone production

As explained in Sect. 3.2, an O_3 difference of about 50 ppbv has been observed by the Falcon aircraft between southwestern and northeastern sides of Cotonou. Southwest side of Cotonou is influenced by air masses from the ocean (see Fig. 1) being advected over the continent where they encounter anthropogenic emissions.

In order to estimate if 50 ppbv of O_3 can be produced by anthropogenic emissions in Cotonou, a chemistry box model was used. CiTTyCAT (Cambridge Tropospheric Trajectory Model of Chemistry and Transport) is a photochemical model including 90 chemical species (see Evans et al. (2000) for details) and has been previously used to simulate chemical evolution in a biomass burning plume originating from Central Africa and advected towards West Africa in the lower-mid troposphere (Real et al., 2010). FLEXPART simulations (see Sect. 4) showed that a large fraction of air masses ending in the O_3 high level plume had remained in the coastal region for about 3 days. A dropsonde launched close to the west profile suggests that this is due to low wind speeds at the altitude of the plume. Meteorological conditions just before the flight were characterised by low winds and no MCS, so it is a reasonable approximation to neglect mixing and wet deposition. Dry deposition is also negligible in this case since the plume was located above 500 m. Therefore a 2-days stationary run was conducted

ACPD
10, 27135–27184, 2010

at Cotonou location.

Since pollutant concentrations directly emitted over the Cotonou/Lagos area and linked to the aircraft data are unknown the model is initialized between 600 and 2000 m with the FF20 observations in the eastern side where the concentrations are typical of a polluted plume. Below and above, CO and NO_x concentrations from the west profile, typical of clean air masses were used. O_3 concentrations from the west profile (clean air masses) were also used for the initialisation. Unfortunately, the aircraft did not measure NO_y and VOC concentrations. VOC initial concentrations are deduced from the mean ratio of VOC/CO measured during the whole campaign by the BAe-146 aircraft in the lower layers (<3 km) scaling the VOC to the CO measured in the high O_3 plume by the FF20. For initialising NO_y, a typical ratio NO_y/NO_x of 2 was used because it is the mean ratio measured during the campaign by the DF20 when encountering high NO_x plumes. NO_z concentrations (NO_y–NO_x) was then partitioned between PAN and HNO_3, with HNO_3 and PAN being respectively 75% and 25% of NO_z. This partitioning corresponds to the values observed in the lower layers during the whole campaign by the BAe-146 aircraft. Concerning water vapour and temperature values, they were taken from the FF20 aircraft and remained constant during the run. A synthesis of the initial conditions used in the run are given in Table 4. Model results of O_3, CO and NO_x mixing ratios after 2 days are shown in Fig. 18. NO_x levels allow the formation of up to 40 ppbv of O_3. The resulting O_3 profile is similar to the measured one from 1–3 km with 2 peaks at 1500 and 2500 m. Peak at 1500 is slightly lower than observed. This can be explained by the likely uncertainties in the initial concentrations. This simulation shows that when using an O_3 profile typical of clean air masses and adding O_3 precursors levels typical of the city emissions, the downwind high O_3 level profile can be simulated with the hypothesis that the plume remains in the same region.

ACPD
10, 27135–27184, 2010

6 Conclusions

Aircraft observations obtained near 3 cities in the altitude range 0–3 km in West Africa during the wet monsoon season are complementary of the O_3 climatology of Thouret et al. (2009) and the BAe aircraft observations recorded around the city of Lagos reported by Hopkins et al. (2009) because they provide a more direct evidence of the role of the African cities in the ozone plume formation.

Near Cotonou O_3 concentrations outside the city plume can be as low as 20 ppbv for air masses advected from the vegetated areas or from the ocean without being under the direct influence of Cotonou or Lagos located further East. Aircraft observations show that an ozone plume can develop with an ozone gradient of 50 ppbv across the plume. A similar behaviour is observed for the Niamey data set although the vertical structure is different with the ozone plume being closer to the ground. For one day (16 August), the ozone gradient across the Niamey plume is also of the order of 50 ppbv. The Cotonou plume is related to a significant increase of NO_x from 1.5 to 5 ppbv. The 1.5 ppbv NO_x level is typical of the clean continental values. No NO_x data are available for 16 August in Niamey, but NO_x observed on 19 August show that elevated concentrations (>3 ppbv) can occurred when crossing the city plume. It is related to a combination of, on one hand, NO_x bare soil emission at the Niamey latitude taking place just after the period 1 to 14 August with significant convective activity over Southwestern Niger, and on the other hand addition of anthropogenic emission from Niamey to exceed the 3 ppbv NO_x concentration level in the plume. The mean NO_x concentrations of the BAe aircraft and the FF20 data outside the city plume shows that at least half of the 3 ppbv NO_x level is related to the soil emission. The Ouagadougou data set is quite different with no ozone plume and it indicates that the absence of a pause in the convective activity and the larger vegetated area around the city prevent ozone plume formation during the wet season.

One of the major question to discuss the ozone increase observed by the aircraft is to separate the large scale biomass burning plume related to transport of emissions

ACPD
10, 27135–27184, 2010

from the SH from the actual influence of the city. This is especially true for the Cotonou/Lagos area where the biomass burning plume is known to be present. Two different approaches have been implemented: a FLEXPART simulation to quantify the probability of transport from the SH compared to air mass stagnation over the emission area and a simulation of the BOLAM model with two different tracers for the anthropogenic emission (RETRO inventory for 2000) and the biomass burning (Liousse et al. (2010) inventory). Both approaches point toward a clear evidence that the ozone increase below the 3-km altitude is related to the city emissions while the ozone maximum above the 3-km altitude is due to the biomass burning emissions. The FLEXPART simulation shows that the air mass stays at least 2 days in the vicinity of the anthropogenic emission. The BOLAM simulation of the PBL structure is in a very good agreement with the meteorological observations (aircraft dropsonde near Cotonou) and shows that this model is well adapted to describe the complex dynamical structure near the coast.

The day to day variability of the transport processes for Niamey and Ouagadougou observations, are based on FLEXPART simulations of the air mass stagnation in the 12° N–14° N latitude band and northward advection of air masses from the vegetated areas influenced by the biogenic VOC emissions. Both conditions need to be fulfilled to be able to detect ozone increase within the city plume. The first condition is necessary to obtain a significant increase of the NO_x concentrations by combining the city emission and the soil emission. It also shows that, contrary to the Niamey conditions, the Ouagadougou air mass transport and its timing respective to the convective activity did not correspond to favourable conditions for O_3 formation during the time period of the aircraft data.

The CittyCAT model simulation does not correspond to a true Lagrangian simulation as in the work of Real et al. (2008), since the initialisation of the concentrations is based on a reconstructed profile using the CO and NO_x observations for the ozone precursors (other species are scaled to these two quantities using mean AMMA observations provided by the DF20 and the BAe-146 aircraft) within the polluted plume and ozone

ACPD
10, 27135–27184, 2010

values corresponding to the background ozone. No mixing neither ozone deposition is included for the Cotonou simulation. Under such conditions, the simulation show that indeed 50 ppbv of ozone can be produced in a two-day period.

Acknowledgements. Based on a French initiative, AMMA was built by an international scientific group and is currently funded by a large number of agencies, especially from France, the UK, the US and Africa. The UMS SAFIRE is acknowledged for supporting the FF20 aircraft deployment and for providing the aircraft meteorological data (humidity and dropsondes). This work was supported by the AMMA EC project and CNRS/INSU. Frank Roux (Laboratoire d'Aérologie) is acknowledged for work on flight planning and validation of the dropsonde data. C. Reeves (UEA Norwich) and the BAe-146 scientific team are acknowledged for the providing the BAe VOC measurements used in the CittyCAT simulation. A. Stohl (NILU) and ECMWF are acknowledged for providing the FLEXPART model and the meteorological analyses..

The publication of this article is financed by CNRS-INSU.

References

Aghedo, A. M., Schultz, M. G., and Rast, S.: The influence of African air pollution on regional and global tropospheric ozone, Atmos. Chem. Phys., 7, 1193–1212, doi:10.5194/acp-7-1193-2007, 2007. 27137

Agusti-Panareda, A., Beljaars, A., Genkova, I., Cardinali, C., and Thorncroft, C.: Impact of assimilating AMMA soundings on ECMWF analyses and forecasts, Tech. rep., ECMWF Technical Memorandum, 2009. 27139, 27150

Ancellet, G., Leclair de Bellevue, J., Mari, C., Nedelec, P., Kukui, A., Borbon, A., and Perros, P.: Effects of regional-scale and convective transports on tropospheric ozone chemistry revealed

ACPD

10, 27135–27184, 2010

by aircraft observations during the wet season of the AMMA campaign, Atmos. Chem. Phys., 9, 383–411, doi:10.5194/acp-9-383-2009, 2009. 27140

Andreae, M. and Merlet, P.: Emission of Trace Gases and Aerosols From Biomass Burning, Global Biogeochem. Cy., 15, 955–966, doi:10.1029/2000GB001382, 2001. 27137

Baehr, J., Schlager, H., Ziereis, H., Stock, P., van Velthoven, P., Busen, R., Strm, J., , and Schumann, U.: Aircraft observations of NO, NO_y CO, and O_3 in the upper troposphere from 60° N to 60° S – Interhemispheric differences at mitlatitudes, Geophys. Res. Lett., 30, 1598–1601, doi:10.1029/2003GL016935, http://dx.doi.org/10.1029/2003GL016935, 2003. 27140

Baumbach, G., Vogt, U., Hein, K. R. G., Oluwole, A. F., Ogunsola, O. J., Olaniyi, H. B., and Akeredolu, F. A.: Air pollution in a large tropical city with a high traffic density – results of measurements in Lagos, Nigeria, Sci. Total Environ., 169, 25–31, doi:10.1016/0048-9697(95)04629-F, 1995. 27137

Chatfield, R. and Delany, A.: Convection Links Biomass Burning to Increased Tropical Ozone: However, Models Will Tend to Overpredict O_3, J. Geophys. Res., 95, 18473–18488, doi:10.1029/JD095iD11p18473, 1990. 27138

Colette, A. and Ancellet, G.: Variability of the tropospheric mixing and of streamer formation and their impact on the lifetime of observed ozone layers, Geophys. Res. Lett., 33, L09808, doi:10.1029/2006GL025793, 2006. 27147

Delon, C., Reeves, C. E., Stewart, D. J., Sera, D., Dupont, R., Mari, C., Chaboureau, J.-P., and Tulet, P.: Biogenic nitrogen oxide emissions from soils - impact on NO_x and ozone over West Africa during AMMA (African Monsoon Multidisciplinary Experiment): modelling study, Atmos. Chem. Phys., 8, 2351–2363, doi:10.5194/acp-8-2351-2008, 2008. 27149

Derognat, C., Beekmann, M., Baeumle, M., Martin, D., and Schmidt, H.: Effect of biogenic volatile organic compound emissions on tropospheric chemistry during the Atmospheric Pollution Over the Paris Area (ESQUIF) campaign in the Ile-de-France region, J. Geophys. Res., 108, 8560–8574, doi:10.1029/2001JD001421, http://dx.doi.org/10.1029/2001JD001421, 2003. 27148

Evans, M. J., Shallcross, D. E., Law, K. S., Wild, J. O. F., Simmonds, P. G., Spain, T. G., Berrisford, P., Methven, J., Lewis, A. C., McQuaid, J. B., Pillinge, M. J., Bandyf, B. J., Penkett, S. A., and Pyle, J. A.: Evaluation of a Lagrangian box model using field measurements from EASE (Eastern Atlantic Summer Experiment) 1996, Atmos. Environ., 34, 3843–3863, doi:10.1016/S1352-2310(00)00184-9, 2000. 27153

Guenther, A., Karl, T., Harley, P., Wiedinmyer, C., Palmer, P. I., and Geron, C.: Estimates

ACPD

10, 27135–27184, 2010

of global terrestrial isoprene emissions using MEGAN (Model of Emissions of Gases and Aerosols from Nature), Atmos. Chem. Phys., 6, 3181–3210, doi:10.5194/acp-6-3181-2006, 2006. 27137

Hopkins, J. R., Evans, M. J., Lee, J. D., Lewis, A. C., H Marsham, J., McQuaid, J. B., Parker, D. J., Stewart, D. J., Reeves, C. E., and Purvis, R. M.: Direct estimates of emissions from the megacity of Lagos, Atmos. Chem. Phys., 9, 8471–8477, doi:10.5194/acp-9-8471-2009, 2009. 27138, 27155

Huntrieser, H., Schumann, U., Schlager, H., Hller, H., Giez, A., Betz, H.-D., Brunner, D., Forster, C., Pinto Jr., O., and Calheiros, R.: Lightning activity in Brazilian thunderstorms during TROCCINOX: implications for NO_x production, Atmos. Chem. Phys., 8, 921–953, doi:10.5194/acp-8-921-2008, 2008. 27137, 27145

Kain, J. S.: The Kain-Fritsch Convective Parameterization: An Update, J. Appl. Meteorol., 43, 170–181, doi:10.1175/1520-0450(2004)043⟨0170:TKCPAU⟩2.0.CO;2, http://journals.ametsoc.org/doi/abs/10.1175/1520-0450%282004%%29043%3C0170%3ATKCPAU%3E2.0.CO%3B2, 2004. 27150

Liousse, C., Guillaume, B., Grégoire, J. M., Mallet, M., Galy, C., Pont, V., Akpo, A., Bedou, M., Castéra, P., Dungall, L., Gardrat, E., Granier, C., Konaré, A., Malavelle, F., Mariscal, A., Mieville, A., Rosset, R., Serça, D., Solmon, F., Tummon, F., Assamoi, E., Yobou, V., and Van Velthoven, P.: Western african aerosols modelling with updated biomass burning emission inventories in the frame of the AMMA-IDAF program, Atmos. Chem. Phys. Discuss., 10, 7347–7382, doi:10.5194/acpd-10-7347-2010, 2010. 27137, 27151, 27156

Malguzzi, P., Grossi, G., Buzzi, A., Ranzi, R., and Buizza, R.: The 1966 "century" flood in Italy: A meteorological and hydrological revisitation, J. Geophys. Res., 111, doi:10.1029/2006JD007111, 2006. 27150

Mari, C. H., Cailley, G., Corre, L., Saunois, M., Attié, J. L., Thouret, V., and Stohl, A.: Tracing biomass burning plumes from the Southern Hemisphere during the AMMA 2006 wet season experiment, Atmos. Chem. Phys., 8, 3951–3961, doi:10.5194/acp-8-3951-2008, 2008. 27139, 27141, 27143

Mauzerall, D. L., Logan, J. A., Jacob, D. J., Anderson, B. E., Blake, D. R., Bradshaw, J. D., Haikes, B., Sachse, G. W., Singh, H., and Talbot, B.: Photochemistry in biomass burning plumes and implications for tropospheric ozone over the tropical South Atlantic, J. Geophys. Res., 103, 8401–8423, doi:10.1029/97JD02612., 1998. 27151

Minga, A., Thouret, V., Saunois, M., Delon, C., Serça, D., Mari, C., Sauvage, B., Mariscal,

ACPD
10, 27135–27184, 2010

A., Leriche, M., and Cros, B.: What caused extreme ozone concentrations over Cotonou in December 2005?, Atmos. Chem. Phys., 10, 895–907, doi:10.5194/acp-10-895-2010, 2010. 27137, 27138, 27149

Parker, D., Burton, R., Diongue-Niang, A., Ellis, R. J., Felton, M., Taylor, C. M., Thorncroft, C. D., Bessemoulin, P., and Tompkins, A. M.: The diurnal cycle of the West African monsoon circulation, Q. J. R. Meteorol. Soc., 131, 2839–2860, doi:10.1256/qj.04.52, http://onlinelibrary.wiley.com/doi/10.1256/qj.04.52/abstract, 2005. 27139

Real, E., Law, K. S., Schlager, H., Roiger, A., Huntrieser, H., Methven, J., Cain, M., Holloway, J., Neuman, J. A., Ryerson, T., Flocke, F., de Gouw, J., Atlas, E., Donnelly, S., and Parrish, D.: Lagrangian analysis of low altitude anthropogenic plume processing across the North Atlantic, Atmos. Chem. Phys., 8, 7737–7754, doi:10.5194/acp-8-7737-2008, 2008. 27156

Real, E., Orlandi, E., Law, K. S., Fierli, F., Josset, D., Cairo, F., Schlager, H., Borrmann, S., Kunkel, D., Volk, C. M., McQuaid, J. B., Stewart, D. J., Lee, J., Lewis, A. C., Hopkins, J. R., Ravegnani, F., Ulanovski, A., and Liousse, C.: Cross-hemispheric transport of central African biomass burning pollutants: implications for downwind ozone production, Atmos. Chem. Phys., 10, 3027–3046, doi:10.5194/acp-10-3027-2010, 2010. 27153

Reeves, C. E., Formenti, P., Afif, C., Ancellet, G., Attié, J.-L., Bechara, J., Borbon, A., Cairo, F., Coe, H., Crumeyrolle, S., Fierli, F., Flamant, C., Gomes, L., Hamburger, T., Jambert, C., Law, K. S., Mari, C., Jones, R. L., Matsuki, A., Mead, M. I., Methven, J., Mills, G. P., Minikin, A., Murphy, J. G., Nielsen, J. K., Oram, D. E., Parker, D. J., Richter, A., Schlager, H., Schwarzenboeck, A., and Thouret, V.: Chemical and aerosol characterisation of the troposphere over West Africa during the monsoon period as part of AMMA, Atmos. Chem. Phys., 10, 7575–7601, doi:10.5194/acp-10-7575-2010, 2010. 27138, 27139, 27141, 27144

Saunois, M., Reeves, C. E., Mari, C. H., Murphy, J. G., Stewart, D. J., Mills, G. P., Oram, D. E., and Purvis, R. M.: Factors controlling the distribution of ozone in the West African lower troposphere during the AMMA (African Monsoon Multidisciplinary Analysis) wet season campaign, Atmos. Chem. Phys., 9, 6135–6155, doi:10.5194/acp-9-6135-2009, 2009. 27144, 27145

Sauvage, B., Gheusi, F., Thouret, V., Cammas, J.-P., Duron, J., Escobar, J., Mari, C., Mascart, P., and Pont, V.: Medium-range mid-tropospheric transport of ozone and precursors over Africa: two numerical case studies in dry and wet seasons, Atmos. Chem. Phys., 7, 5357–5370, doi:10.5194/acp-7-5357-2007, 2007. 27149

Sauvage, B., Martin, R., van Donkelaar, A., and Ziemke, J.: Quantification of the fac-

ACPD

10, 27135–27184, 2010

tors controlling tropical tropospheric ozone and the South Atlantic maximum, J. Geophys. Res., 112, D11309–D11322, doi:10.1029/2006JD008008, http://dx.doi.org/10.1029/2006JD008008, 2007b. 27138

Schultz, P.: An Explicit Cloud Physics Parameterization for Operational Numerical Weather Prediction, Mon. Weather Rev., 123, 3331–3343, doi:10.1175/1520-0493(1995)123⟨3331:AECPPF⟩2.0.CO;2, 1995. 27150

Schumann, U. and Huntrieser, H.: The global lightning-induced nitrogen oxides source, Atmos. Chem. Phys., 7, 3823–3907, doi:10.5194/acp-7-3823-2007, 2007. 27137

Stohl, A., Hittenberger, M., and Wotawa, G.: Validation of the lagrangian particle dispersion model FLEXPART against large-scale tracer experiment data, Atmos. Environ., 32, 4245–4264, doi:10.1016/S1352-2310(98)00184-8, 1998. 27146

Stohl, A., Eckhardt, S., Forster, C., James, P., Spichtinger, N., and Seibert, P.: A replacement for simple back trajectory calculations in the interpretation of atmospheric trace substance measurements, Atmos. Environ., 36, 4635–4648, doi:10.1016/S1352-2310(02)00416-8, http://www.sciencedirect.com/science/article/B6VH3-46PBJBX-8/%2/7d8c7b6557524176d31e8d96169cd1df, 2002. 27146

Thompson, A., Doddridge, B., Witte, J., Hudson, R., Luke, W., J.E.Johnson, Johnson, B., Oltmans, S., and Weller, R.: A tropical Atlantic paradox: Shipboard and satellite views of a tropospheric ozone maximum and wave-one in January-February 1999, Geophys. Res. Lett., 27, 2000. 27138

Thouret, V., Saunois, M., Minga, A., Mariscal, A., Sauvage, B., Solete, A., Agbangla, D., Nédélec, P., Mari, C., Reeves, C. E., and Schlager, H.: An overview of two years of ozone radio soundings over Cotonou as part of AMMA, Atmos. Chem. Phys., 9, 6157–6174, doi:10.5194/acp-9-6157-2009, 2009. 27137, 27138, 27141, 27153, 27155, 27168

Tompkins, A., Diongue-Niang, A., Parker, D., and Thorncroft, C. D.: The African easterly jet in the ECMWF Integrated Forecast System: 4D-Var analysis, Q. J. R. Meteorol. Soc., 131, 2861–2885, doi:10.1256/qj.04.136, http://onlinelibrary.wiley.com/doi/10.1256/qj.04.136/abstract%, 2005. 27139

Vizy, E. K. and Cook, K. H.: Development and application of a mesoscale climate model for the tropics: Influence of sea surface temperature anomalies on the West African monsoon, J. Geophys. Res., 107, 4023–4044, doi:10.1029/2001JD000686, 2002. 27149

Williams, J. E., Scheele, R., van Velthoven, P., Bouarar, I., Law, K., Josse, B., Peuch, V.-H., Yang, X., Pyle, J., Thouret, V., Barret, B., Liousse, C., Hourdin, F., Szopa, S., and Cozic,

ACPD
10, 27135–27184, 2010

A.: Global Chemistry Simulations in the AMMA Multimodel Intercomparison Project, Bull. Am. Meteorol. Soc., 91, 611–624, doi:10.1175/2009BAMS2818.1, http://journals.ametsoc.org/doi/abs/10.1175/2009BAMS2818.1, 2010. 27153

Zampieri, M., Malguzzi, P., and Buzzi, A.: Sensitivity of quantitative precipitation forecasts to boundary layer parameterization: a flash flood case study in the Western Mediterranean, Natural Hazards and Earth System Science, 5, 603–612, doi:10.5194/nhess-5-603-2005, http://www.nat-hazards-earth-syst-sci.net/5/603/2005/, 2005. 27150

ACPD

10, 27135–27184, 2010

Table 1. List of the FF20 flights near Niamey.

Day (UTC)	Takeoff UTC	Landing UTC	Species measured
11 August		15:30	CO^{l}
13 August	12:15	15:30	O_3, CO^{t}
14 August	06:30	09:30	O_3^{l}
15 August	12:30	15:45	O_3^{t}, CO^{t}
16 August	14:00	18:00	O_3, CO^{t}
17 August	09:00	12:00	O_3, CO^{t}
19 August	09:15	16:30	O_3^{l}, NO_x, CO^{l}
20 August	14:00	17:30	O_3, NO_x, CO

^{t} measured during takeoff only
^{l} measured during landing only

ACPD
10, 27135–27184, 2010

Table 2. List of the DF20 flights near Ouagadougou.

Day (UTC)	Takeoff UTC	Landing UTC	Species measured
1 August		11:30	O_3, NO_x, CO
4 August	08:45	12:15	O_3, NO_x, CO
6 August	09:30	12:45	O_3, NO_x, CO
7 August	12:20	15:15	O_3, NO_x, CO
11 August	14:50	17:50	O_3, NO_x, CO
13 August	10:40	14:00	O_3, NO_x, CO
15 August	09:15	12:30	O_3, NO_x, CO
15 August	14:30	17:00	O_3, NO_x, CO

ACPD
10, 27135–27184, 2010

Table 3. List of the MCS near Niamey or Ouagadougou.

Day	Position	Comments on MCS evolution
31 July	2.5° W, 15° N	Travelling over Ouagadougou at 16:30 UT and growing during the day
4 August	2.5° W, 14° N	North of Ouagadougou in the morning, decays after 09:00 UT but cloudy in the afternoon
6 August	2° E, 13° N	Large MCS travelling west over Ouagadougou after 12:00 UT
7 August	2° E, 13° N	A patchy MCS develops over Ouagadougou after 15:00 UT
11 August	3° E, 13° N	Large MCS over Niamey in the morning and Ouagadougou after 12:00 UT
14 August	2° E, 14° N	MCS arriving over Niamey at 12:00 UT and decays during the day
16 August	2° W, 12° N	Small system developing over Ouagadougou during the day
17 August	2° E, 15° N	Small system forming North of Niamey, decays during the day but cloudy in Niamey until 14:00 UT

ACPD
10, 27135–27184, 2010

Table 4. Chemical initialisation of the box model run. The origin of the chosen concentrations is indicated. When no indication are given, FF20 stands for polluted plume profile (east profile). Bae-146 measurements in the lower layers for all the campaign were scaled to FF20 CO measurement. The following NMVOC were initialised : MeCHO, Me_2CO, C_2H_2, C_6H_6, C_4H_{10}, C_4H_8, C_2H_6, C_2H_4, isoprene, C_5H_{12}, C_3H_8, C_3H_6, C_7H_8, $HONO_2$.

Species	Origin	Species	Origin
CO	FF20	H_2O_2	FF20 west profile
O_3	FF20 west profile	CH_4	1.75 ppm
NO_x	FF20	NMVOC	BAe-146
HCHO	BAe-146	NO_y	NO_x FF20 and DF20 NO_y/NO_xratio
PAN	25% of NO_y-NO_x	HNO_3	75% of NO_y-NO_x

ACPD
10, 27135–27184, 2010

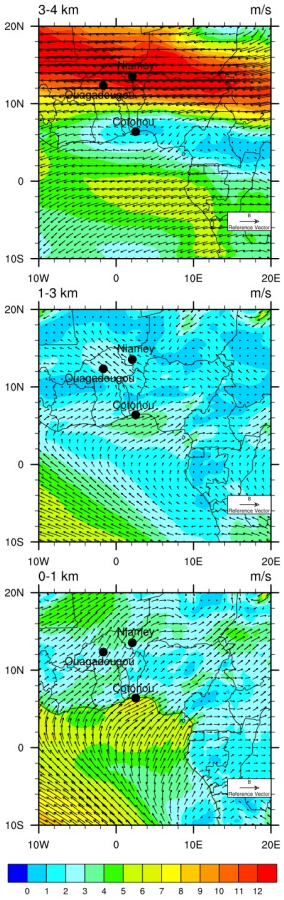

Fig. 1. Wind velocity (m/s) and vectors from ECMWF reanalysis averaged over August 2006 for the 3–4 km (top), 1–3 km (middle) and 0–1 km tropospheric layers.

ACPD
10, 27135–27184, 2010

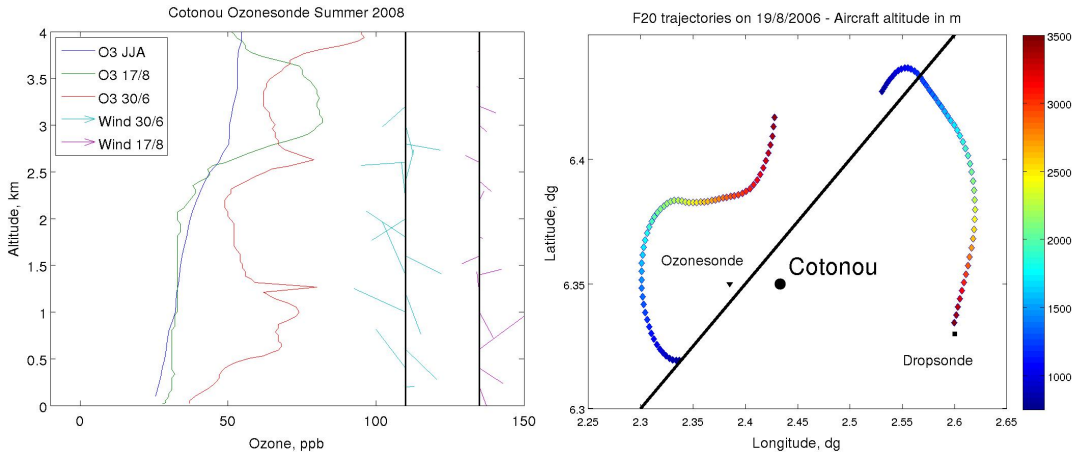

Fig. 2. (Left panel) Three O_3 mixing ratio vertical profiles in ppbv measured by the Cotonou ozone sonde station Thouret et al. (2009), the location of which is plotted on the right panel map: the 2006 June/July/August mean, the 17 August and 30 June 2006. Wind vector vertical profiles are shown for 17 and 30 August (the base of the wind vector is on the solid line). (Right panel) Map of the aircraft positions when flying between 750 m and 3500 m around Cotonou on 19 August. The color scale is the aircraft altitude. The aircraft position when launching the 10:41 UT dropsonde is shown. The black solid line separates the ozone rich (East) and poor (West) area shown in Fig. 3.

ACPD
10, 27135–27184, 2010

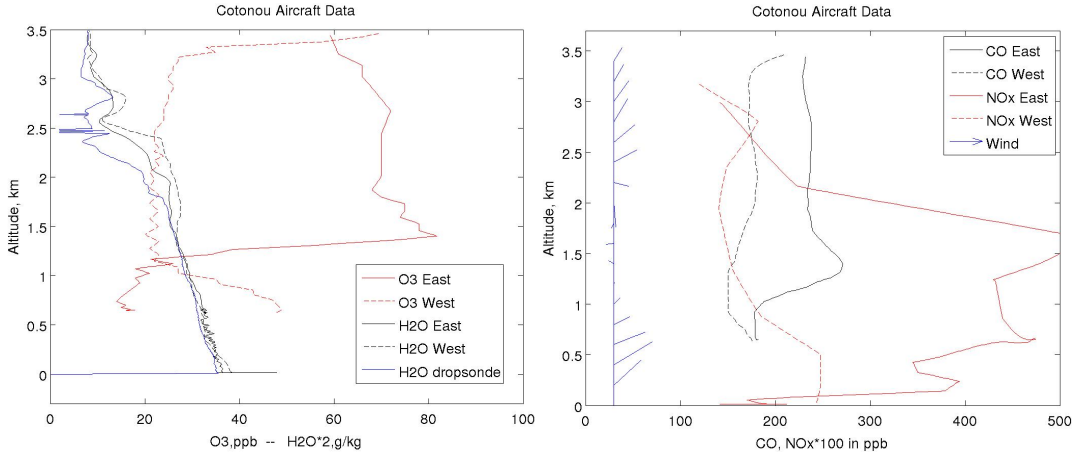

Fig. 3. The O_3, H_2O (left panel) and CO, NO_x (right panel) vertical profiles measured by the FF20 on August 19 West and East of Cotonou (see Fig. 2). H_2O mixing ratio is in g/kg and O_3, NO_x, and CO mixing ratios are in ppbv. The H_2O dropsonde vertical profiles (left panel) describes the PBL evolution between 10:45 UT and 13:45 UT. The dropsonde vertical profiles of the wind direction (right panel) shows the weakening of the southeasterly flow in the ozone rich altitude range. The base of the wind vector is on the solid line.

ACPD
10, 27135–27184, 2010

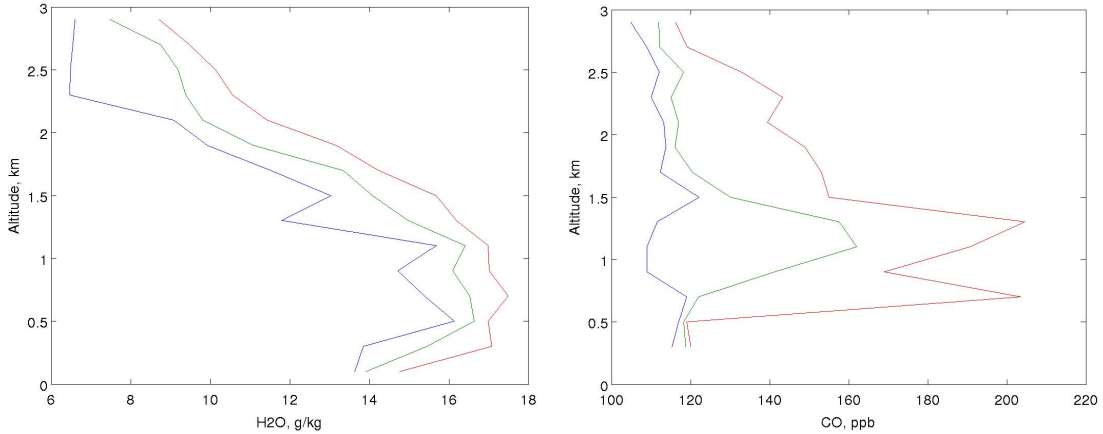

Fig. 4. Vertical profiles of the 25th, 50th and 75th percentile of the H_2O mass mixing ratio in g/kg (left panel) and CO mixing ratio in ppbv (right panel) for the 15 Niamey takeoff and landing of the FF20 (only 8 profiles for CO).

ACPD
10, 27135–27184, 2010

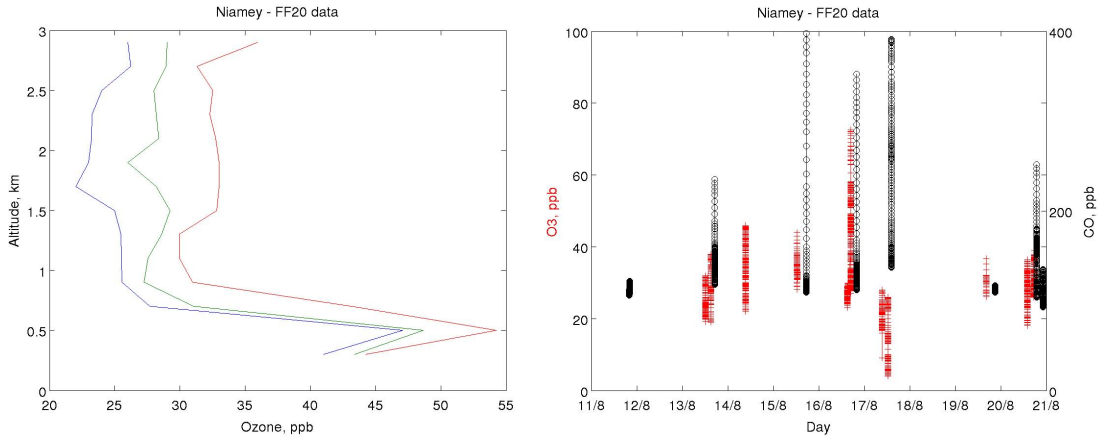

Fig. 5. Vertical profiles of the 25th, 50th and 75th percentile of the O_3 mixing ratio in ppbv (left panel) and daily variability of O_3 (red) and CO (black) mixing ratio range in ppbv measured in the 0–3 km altitude range (right panel) for the 10 (O_3) and 8 (CO) takeoff and landing of the FF20.

ACPD
10, 27135–27184, 2010

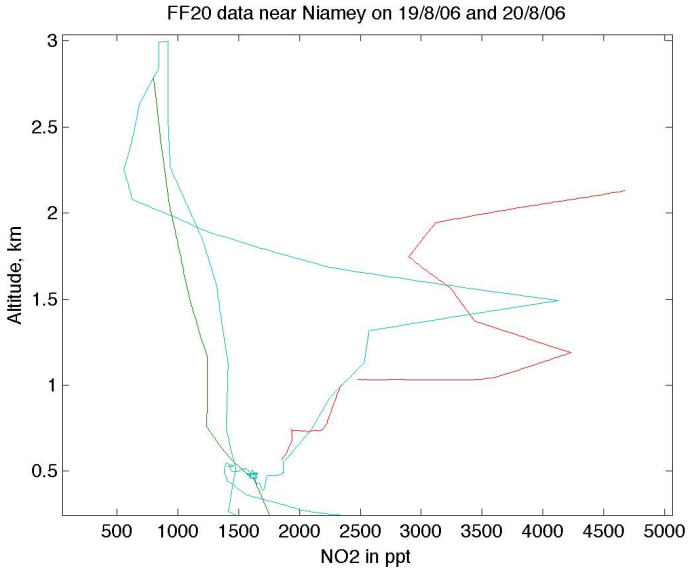

Fig. 6. Vertical profiles of the NO_x mixing ratio in ppbv measured by the FF20 on 19 August (green and red) and 20 (blue). Larger concentrations correspond to landing profiles.

ACPD
10, 27135–27184, 2010

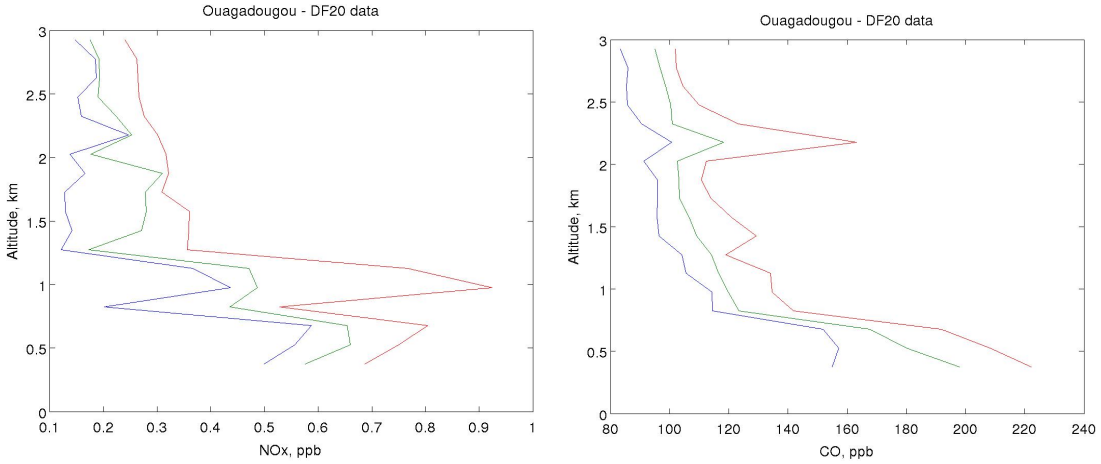

Fig. 7. Vertical profiles of the 25th, 50th and 75th percentile of the NO_x (left panel) and CO mixing ratio in ppbv (right panel) for the 15 Ouagadougou takeoff and landing of the DF20.

ACPD
10, 27135–27184, 2010

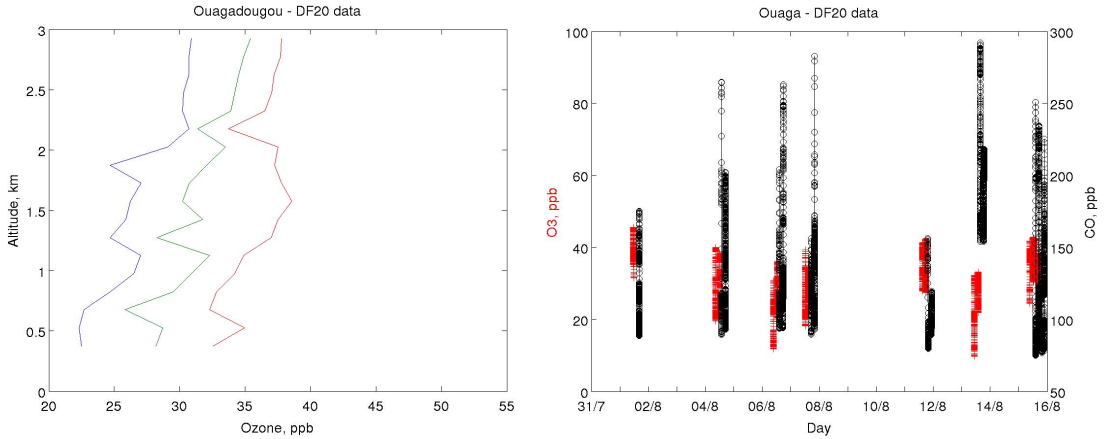

Fig. 8. Vertical profiles of the 25th, 50th and 75th percentile of the O_3 mixing ratio in ppbv (left panel) and daily variability of O_3 (red) and CO (black) mixing ratio range in ppbv measured in the 0–3 km altitude range (tight panel) for the 15 Ouagadougou takeoff and landing of the DF20.

ACPD
10, 27135–27184, 2010

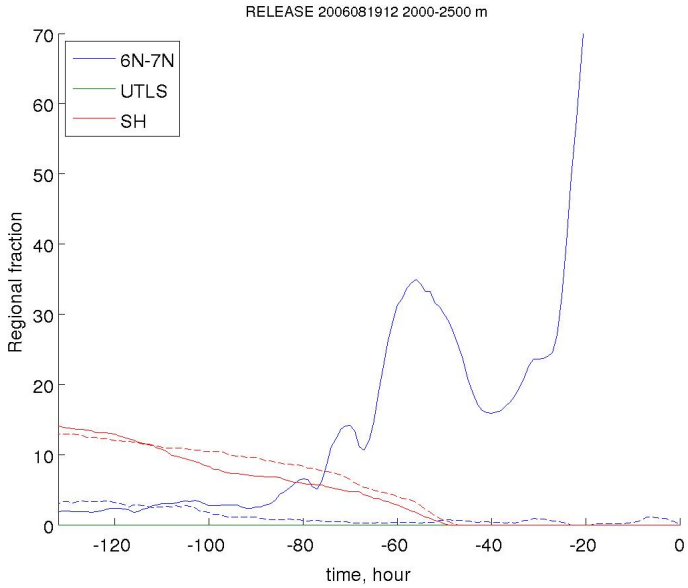

Fig. 9. Fraction of particles being in 3 different regions (see text for the definition of the regions) at each time step of FLEXPART simulations for two releases above Cotonou: altitude 2250 m (solid line) and 3750 m (dotted line). The UTLS fraction is always negligible.

ACPD
10, 27135–27184, 2010

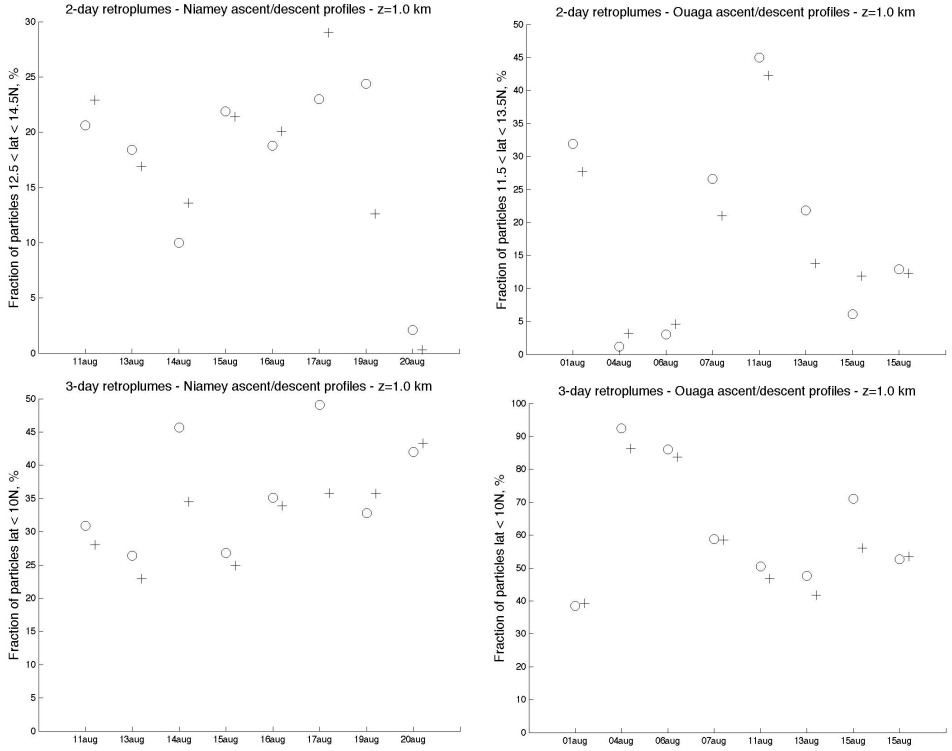

Fig. 10. Daily variability of the results of a backward FLEXPART run for a release at 1 km above Niamey (right column) and Ouagadougou (left column) for every flight of the FF20 and DF20 at time t0. Top row panel is the fraction of particles remaining within the 1°latitude band around Niamey at t0-1 days. Bottom row is the fraction of particles coming from latitudes < 10° N at t0–2 days.

ACPD
10, 27135–27184, 2010

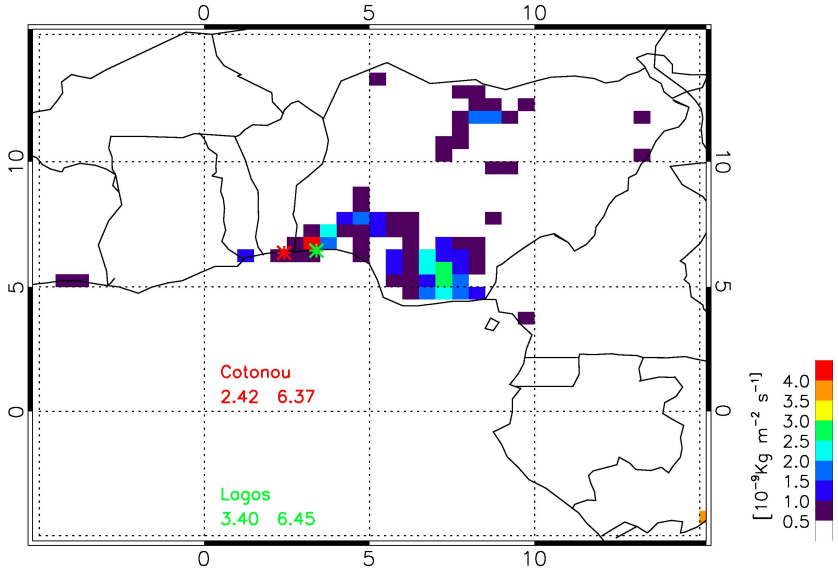

Fig. 11. RETRO CO emissions for August 2000.

ACPD
10, 27135–27184, 2010

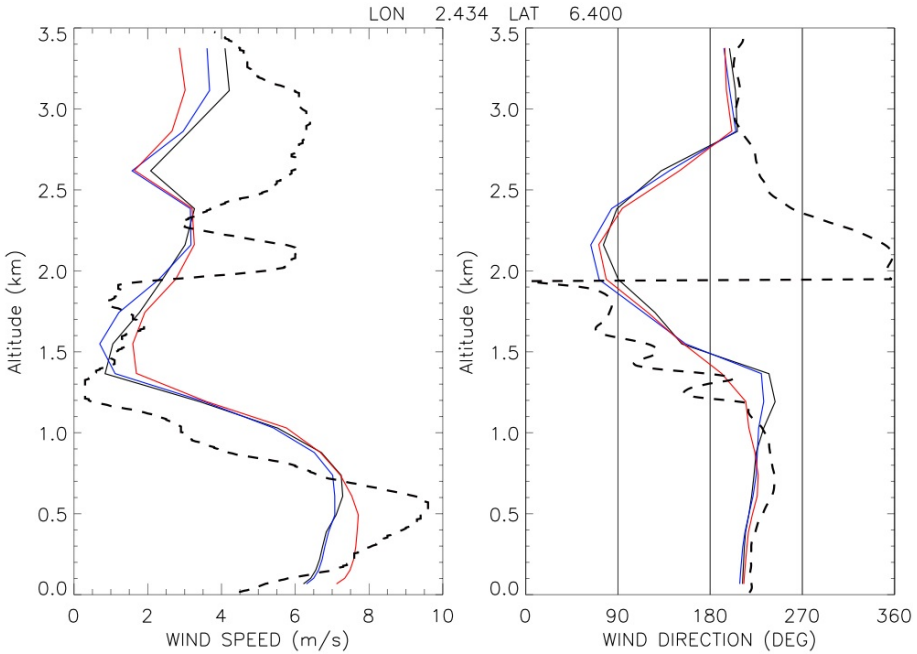

Fig. 12. Wind speed and wind direction from dropsonde launched at 10:40 UTC (black dashed) and from BOLAM simulation with 7 km horizontal resolution at 10:00 UTC (black), 12:00 UTC (blue) and 14:00 UTC on 19 August (red) over Cotonou.

ACPD
10, 27135–27184, 2010

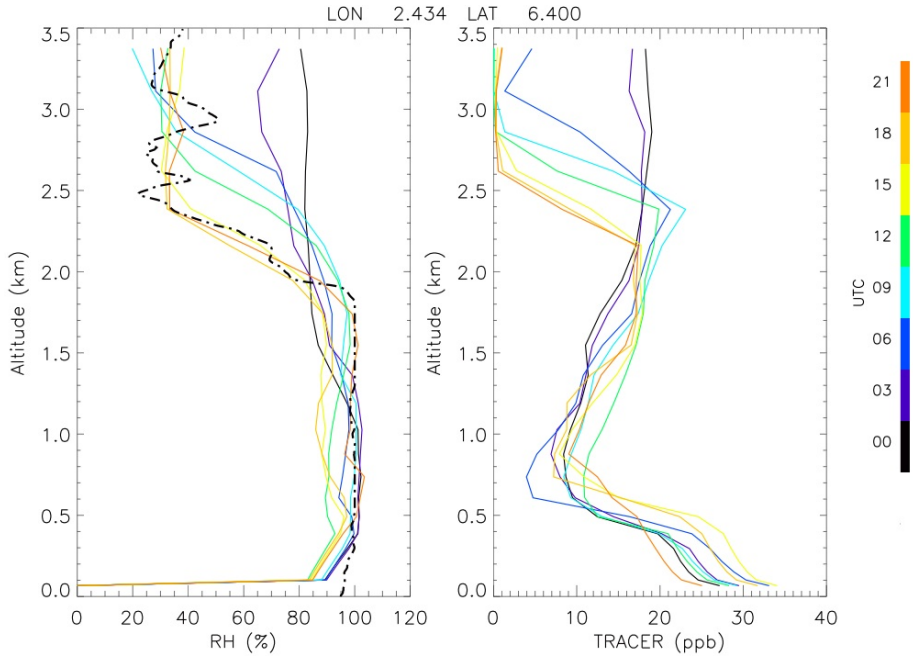

Fig. 13. Time evolution of relative humidity and anthropogenic tracer concentration in ppbv over Cotonou from BOLAM simulation with 7 km horizontal resolution. Black dashed line is relative humidity from dropsonde launched at 10:41 UTC.

ACPD
10, 27135–27184, 2010

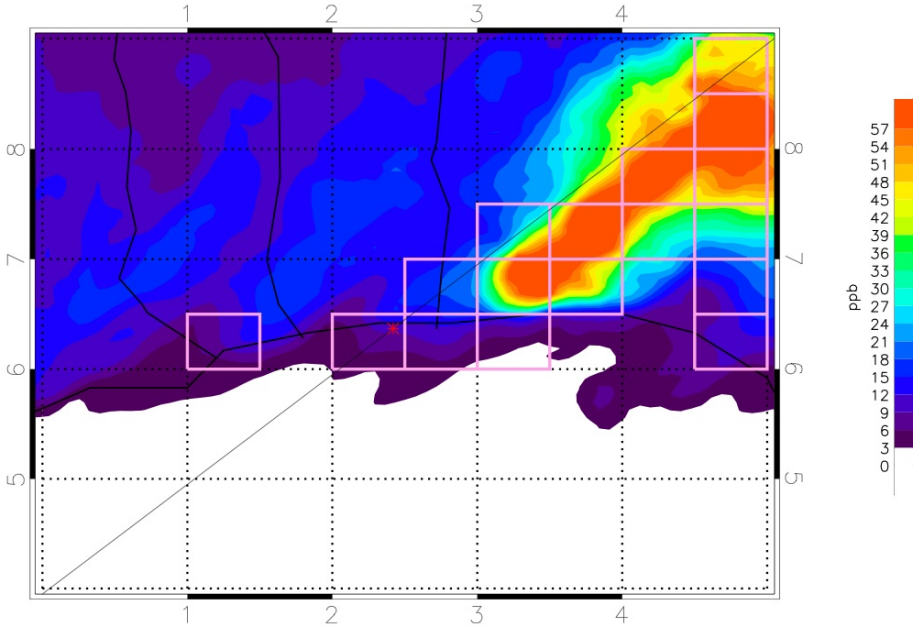

Fig. 14. Horizontal cross section at 900 hPa of anthropogenic tracer concentration in ppbv on 19 August, 13:00 UTC from BOLAM simulation with 7 km horizontal resolution. Solid line indicates the position of the vertical cross section in Fig. 15. The position of Cotonou is indicated by the red asterisk. Pink squares indicate where CO emissions are greater then 0.5 µg/m^2/s.

ACPD
10, 27135–27184, 2010

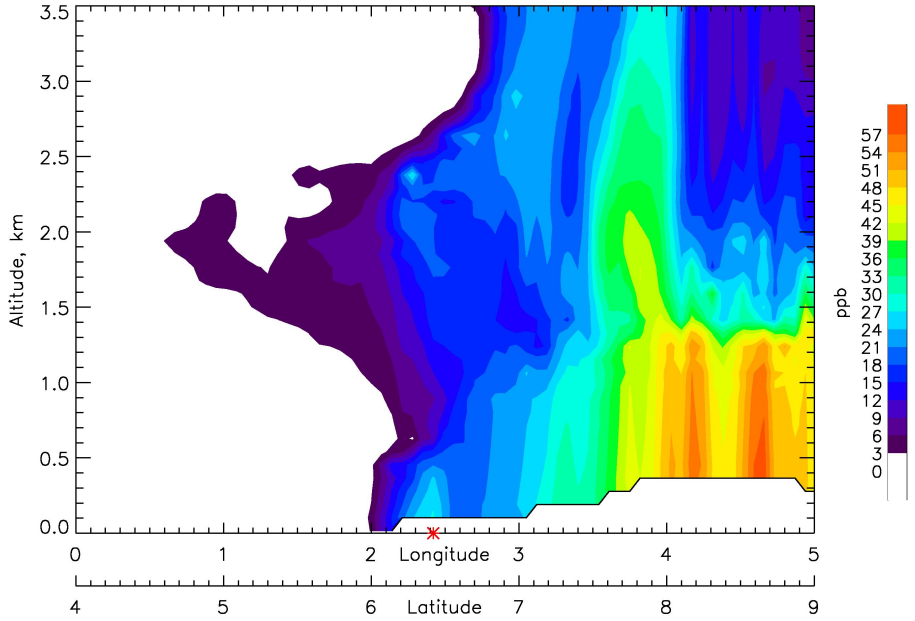

Fig. 15. Vertical cross section of anthropogenic tracer concentration in ppbv on 19 August, 12:00 UTC from BOLAM simulation with 7 km horizontal resolution. The position of Cotonou is indicated by the red asterisk.

ACPD
10, 27135–27184, 2010

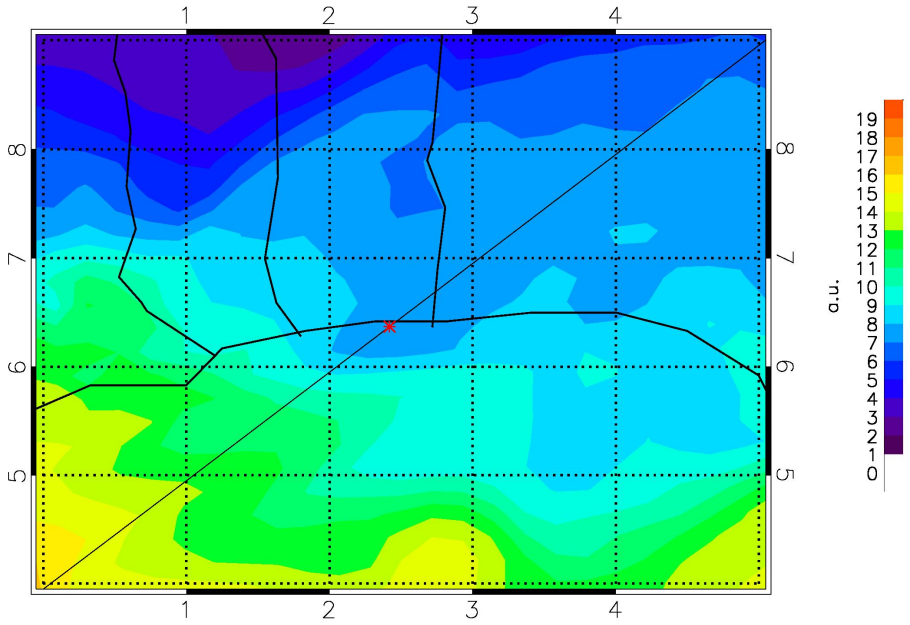

Fig. 16. Horizontal cross section at 900 hPa of biomass burning tracer concentration on August 19, 12 UTC from BOLAM simulation with 24 km horizontal resolution. Solid line indicates the position of the vertical cross section in Fig. 17. The position of Cotonou is indicated by the red asterisk.

ACPD
10, 27135–27184, 2010

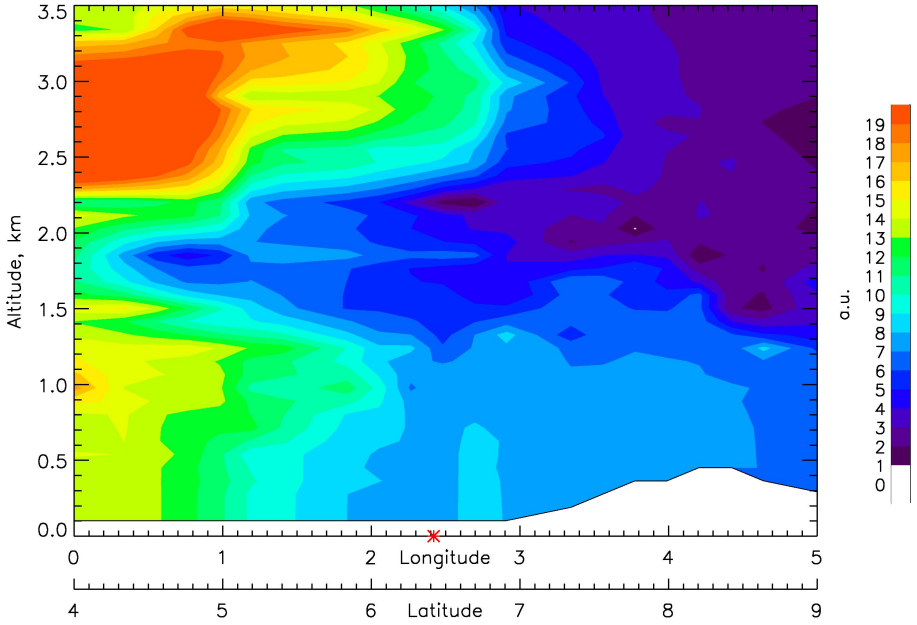

Fig. 17. Vertical cross section of biomass burning tracer concentration on 19 August, 12:00 UTC from BOLAM simulation with 24 km horizontal resolution. The position of Cotonou is indicated by the red asterisk.

ACPD
10, 27135–27184, 2010

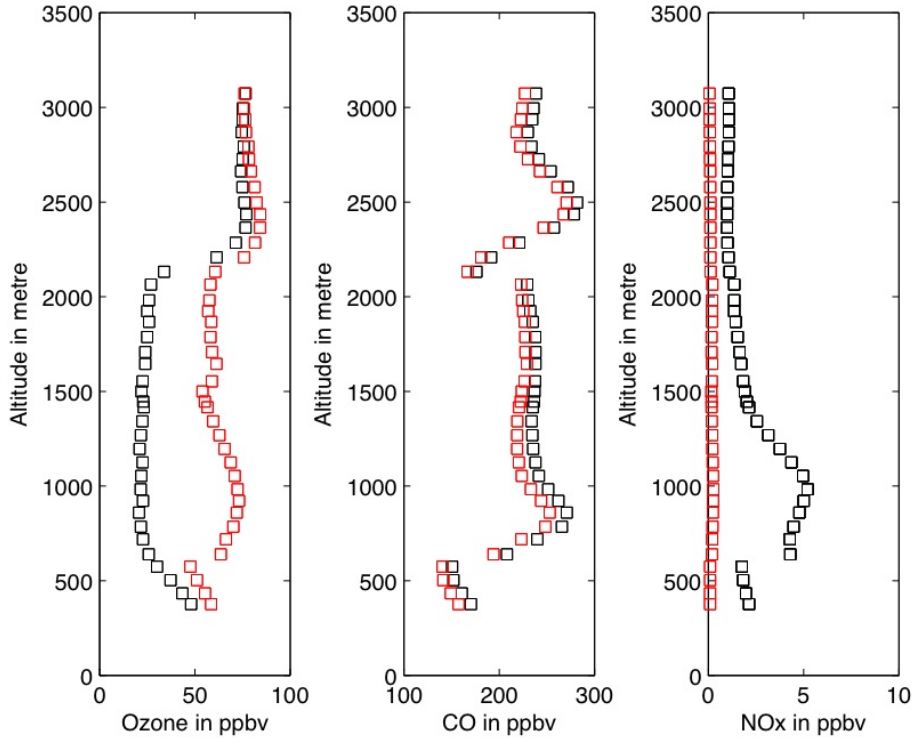

Fig. 18. CittyCat simulation of the Cotonou plume. O_3, CO and NO_x profiles simulated upwind and downwind the city are shown in black and red respectively.

ACPD
10, 27135–27184, 2010